

Fringe pattern photobleaching, a new method for the measurement of transport coefficients of biological macromolecules

Jean Davoust*, Philippe F. Devaux, and Liliane Leger¹

Institut de Biologie Physico Chimique, 13 rue Pierre et Marie Curie, 75005 Paris, and ¹Laboratoire de Physique de la Matière Condensée, Collège de France, 75231 Paris Cedex, France

Communicated by L. De Maeyer
Received on 18 August 1982

The conventional method of studying mass transport in membranes by spot photobleaching and then following the recovery of fluorescence has disadvantages. Among them, the need for a high density of fluorescent molecules, the measurement of the beam profile, and a knowledge of the photobleaching processes are of a crucial importance. The application of a planar fringe pattern of light both for the bleaching and the monitoring of the fluorescent molecules solves these three major difficulties. Brownian diffusion coefficients and flow velocities can be measured independently and are averaged over the whole fringe pattern volume. These transport coefficients are explored over the wide range of experimentally accessible distances (from an interfringe spacing 0.5–50 μm). The quantification of the mobile and immobile components is further simplified by scanning the fringe pattern and detecting only a modulated fluorescence recovery signal. The fringe pattern photobleaching method is particularly adapted to the measurements of diffusion coefficients and flow velocity of membrane components, as well as of cytoplasmic proteins. The theoretical results and the test experiments with fluorescent bovine serum albumin are described.

Key words: diffusion/flow velocity/fringe pattern/photobleaching

Introduction

The lateral motions and the distributions of molecules in membranes play significant roles in cellular metabolism. Lateral mobility is particularly involved in the formation of heterogeneous regions on a cell surface, during membrane surface endocytosis and recycling (Matlin *et al.*, 1981) in synaptic spot formation (Axelrod *et al.*, 1976a), and specific ligand-receptor recognition (Dragsten *et al.*, 1979).

New techniques have emerged to measure the translational mobility of fluorescent molecules within cell plasma membranes (Peters *et al.*, 1974; Edidin *et al.*, 1976) or artificial membrane preparations (Schindler *et al.*, 1980). One of the methods is based on the photobleaching of the fluorescent molecules in a small area of the sample and the subsequent observation of the recovery of fluorescence in that area (Axelrod *et al.*, 1976b). Fluorescence recovery after photobleaching can also be applied to the study of the mobility of molecules within the cytoplasm of living cells (Wojcieszyn *et al.*, 1981) and to the diffusion of biopolymers in solution (Lanni *et al.*, 1981). This elegant technique (recently reviewed by Peters, 1981) is limited in its applications because of factors such as the beam damage to the cell, the limit in the density of detectable molecules (10^3 – 10^4 molecules/μm²), the

assumed first order rate constant of the photobleaching reaction, and the necessity for the intensity of the incident beam to have a well defined profile.

In the present article, we describe an improved version of this method: using a sinusoidal profile (fringe pattern) of light, accurate transport coefficients can be determined with a high sensitivity. The method of periodic pattern photobleaching (introduced by Smith and McConnell, 1978; Smith *et al.*, 1979) shares some of the advantages discussed here. Their procedure needs real-time image recordings combined with a data processing system. Here we propose three basic modifications of the Smith-McConnell procedure: (1) the photobleaching light pulse is produced by two interfering high intensity laser beams; (2) the detection also uses interference fringes with the same periodicity; (3) the position of this attenuated fringe pattern (but not its amplitude) is varied by mechanical vibration of a mirror. A photomultiplier associated with a lock-in amplifier measures the relaxing amplitude of the fluorescence concentration profile.

The procedure was tested by measuring the diffusion of bovine serum albumin (BSA), labelled with fluorescein isothiocyanate (FITC), in water-glycerol solution. In this paper we discuss the simulation of the data and the attainable signal-to-noise ratio, together with the design of the instrument.

Results

Theoretical results

Transport properties of a given fluorescent species are obtained from the observation of the relaxation of a non-uniform concentration profile. For Brownian diffusion the concentration of fluorescent molecules in a three-dimensional medium can be described by the mass diffusion equation:

$$\frac{\partial}{\partial t} c(\vec{r}, t) = D \nabla^2 c(\vec{r}, t) \quad (1)$$

where $c(\vec{r}, t)$ is the concentration of fluorophore at time t in a small volume around coordinate x, y, z of a vector \vec{r} . D is an isotropic lateral diffusion coefficient. Assuming an infinite medium, a Fourier transform of eq. (1) gives:

$$\frac{\partial}{\partial t} C(\vec{q}, t) = -Dq^2 C(\vec{q}, t) \quad (2)$$

with $C(\vec{q}, t) = (2\pi)^{-3/2} \int c(\vec{r}, t) \exp(j\vec{q}\cdot\vec{r}) d^3r$. The solution of (2) is:

$$C(\vec{q}, t) = C(\vec{q}, 0) \exp(-Dq^2 t) \quad (3)$$

where $C(\vec{q}, 0)$ is the initial concentration of fluorescent molecules in the Fourier space immediately after photobleaching. The total fluorescence intensity emitted by the sample, when excited with a monitoring beam of intensity profile $I(\vec{r})$, is proportional to $F(t)$:

$$F(t) = \int c(\vec{r}, t) I(\vec{r}) d^3r = \int C(\vec{q}, t) I(-\vec{q}) d^3q \quad (4)$$

where $I(-\vec{q}) = (2\pi)^{-3/2} \int I(\vec{r}) \exp(-j\vec{q}\cdot\vec{r}) d^3r$.

Combining equations (3) and (4) we find the general expression of the fluorescence recovery signal in any photobleaching experiment:

*To whom reprint requests should be sent.

$$F(t) = \int \exp(-Dq^2t)C(\vec{q},0)I(-\vec{q})d^3q \quad (5)$$

The knowledge of the beam profile $I(\vec{r})$ is required to determine the terms $I(-\vec{q})$. On the other hand, the order of the photobleaching reaction associated with the bleaching light intensity creates the initial distribution of $C(\vec{q},0)$. Both terms are important for deducing the diffusion coefficient D from $F(t)$ (for a detailed analysis, see Axelrod *et al.*, 1976b). Instead of $F(t)$, one can measure the terms $C(\vec{q},t)$ from numerical Fourier transforms of time-lapsed recorded images (Smith *et al.*, 1979).

We propose a simplification of this method, in which a real fringe pattern with interfringe spacing i is formed in the volume of two crossing coherent laser beams. These planar interference fringes provide a way of producing a light intensity profile which in fact contains two Fourier components: one for $|\vec{q}| = 0$ (mean incident light level) and one for a fixed wave vector ($|\vec{q}_0| = 2\pi/i$) lying along an axis normal to the fringe planes (spatially modulated light level). Thus, the fluorescence intensity signal is a superposition of a constant component $C(0,0)$ and a purely exponential decaying component associated with the wave vector \vec{q}_0 : $\exp(-Dq_0^2t)C(\vec{q}_0,0)$. The contrast obtained in the experiment (i.e., the ratio of the relaxing part of the fluorescent intensity to the constant part) will be dominated by two quantities: (1) the initial concentration profile at wave vector \vec{q}_0 : $C(\vec{q}_0,0)$; (2) the spatial distribution of the observation light $I(-\vec{q})$. We shall further consider separately those two quantities.

Influence of the initial concentration profile of fluorescent molecules. Obviously, it is an advantage to start with a concentration profile modulated at the particular wave vector \vec{q}_0 . To simplify the description, we suppose that the bleaching pulse is composed of an infinite number of planar interference fringes and these are normal to the x axis. The light intensity profile is given by:

$$I(\vec{r}) = I_b [1 + \cos(\vec{q}_0 \cdot \vec{x})] \quad (6)$$

where I_b is the mean level of the bleaching light intensity. The corresponding initial concentration profile is not obvious. It depends upon the sequence of chemical reactions, as well as upon the duration and intensity of the incident light. It is usually a difficult task to test these initial conditions experimentally for each sample. Many of the methods for calibrating the experiment (beam size, order of the photochemical reaction, etc.) have already been discussed (Axelrod *et al.*, 1976b). For a first order reaction, induced by a pulse whose duration (Δt) is much shorter than the characteristic diffusional time constant, the initial distribution is described by: $c(\vec{r},0) = c_0 \exp(-\alpha I(\vec{r})t)$ where α is the first order photolytic reaction rate constant and $I(\vec{r})$ the light intensity profile of equation (6). Thus the complete equation becomes:

$$c(\vec{r},0) = c_0 \exp[-K(1 + \cos(\vec{q}_0 \cdot \vec{x}))] \quad (7)$$

where $K = \alpha I_b \Delta t$ is the mean bleaching efficiency index (Axelrod *et al.*, 1976b). In Figure 1 the initial concentration profiles $c(r,0)$ are shown for different K values.

As can be seen from equation (5), the important determinants for the analytical solution of the fluorescence recovery signal are the Fourier components $A_n(K,0)$ of $c(\vec{r},0)$. For an infinite number of fringes, the concentration profile is expanded in the following Fourier series:

$$c(\vec{r},t) = c_0 \sum_{n=-\infty}^{n=\infty} A_n(K,t) \exp(jn\vec{q}_0 \cdot \vec{x}) \quad (8)$$

The initial Fourier coefficients $A_n(K,0)$ can be calculated

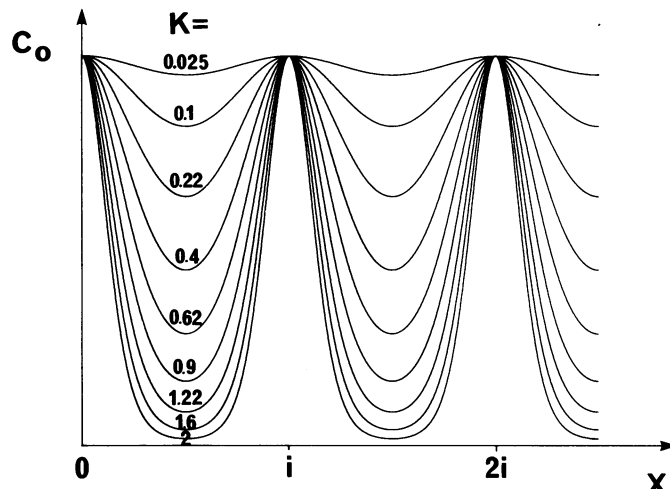


Fig. 1. Simulation of the concentration profile of fluorescent molecules immediately following the bleaching pulse. A first order photolytic reaction was achieved by an incident light intensity profile sinusoidally modulated in one direction. The curves correspond to different photobleaching efficiencies K , as defined in the text.

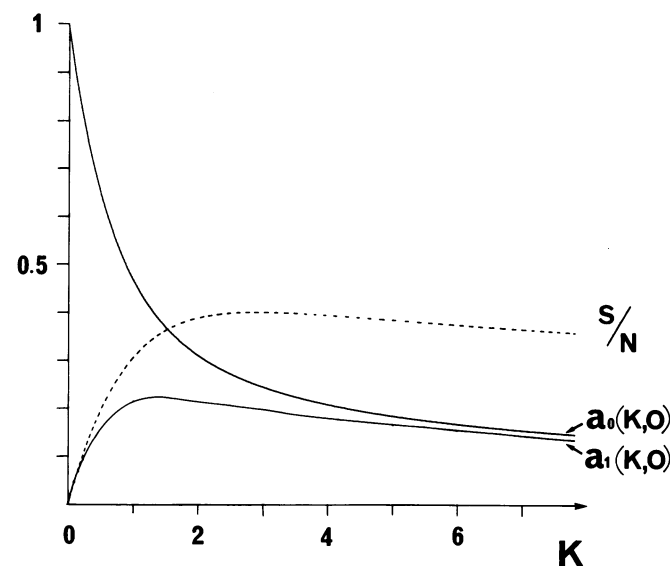


Fig. 2. Plot of two Fourier components of the concentration profile of fluorescent molecules just after receiving the bleaching light pulse. A first order photobleaching reaction was used and the components are plotted as a function of the photobleaching efficiency K . $A_0(K,0)$ is the component at zero wave-vector, and represents the average concentration of the fluorophores (base line). $A_1(K,0)$ is the component at wave vector $q_0 = 2\pi/i$, where i is the interfringe spacing of the bleaching light profile. The dotted line represents the signal-to-noise ratio of the experiment for $A_1(K,0)/(A_0(K,0))^{-1/2}$, $B = 1$ see equation (12).

(Schwartz, 1965) from an expansion of eq. (7), giving $A_n(K,0) = (-1)^n I_n(K) \exp(-K)$, where $I_n(K)$ is a modified Bessel function $I_n(K) = \sum_{m=0}^{\infty} (K/2)^{(n+2m)} [n!(m+n)!]^{-1}$.

In Figure 2 we show how the coefficients $A_0(K,0)$ and $A_1(K,0)$ vary as a function of K ; these two coefficients represent, respectively, the mean concentration in fluorescent molecules and the amplitude of the fluorescence at wave vector q_0 just after the bleaching pulse. This latter has one maximum: $A_1(K,0) = 0.22$ for $K = 1.5$. By combining equation (8) with equation (1), we have:

$$A_n(K, t) = A_n(K, 0) \exp(-n^2 q_0^2 t) \quad (9)$$

Other reaction schemes (possibly having orders of reaction > 1) or different bleaching times, Δt , affect only the explicit expressions of the initial coefficients $A_n(K, 0)$ with the same time dependence for each spatial component $A_n(K, t)$.

Influence of the monitoring beam intensity profile upon the fluorescence recovery signal. The sine profile of the fringe pattern performs a real time Fourier transform of the fluorescence concentration profile. If ϕ denotes the spatial phase shift between the intense fringe pattern (which bleaches the fluorophore) and the attenuated (I_0) measuring fringe pattern, then the final monitoring light intensity profile is given by $I_{\text{mon}}(r) = I_0[1 + \cos(\vec{q}_0 \cdot \vec{x} + \phi)]$. Combining equations (4), (5), and (9) gives the following fluorescence signal:

$$F(t) = I_0 C_0 [A_0(K, 0) + A_1(K, 0) \exp(-Dq_0^2 t) \cos \phi] \quad (10)$$

This is the solution of equation (5) for an infinite fringe pattern. Of course, the finite size of the beam reduces the number of fringes N ($N = \pi w / i$, where w is the e^{-2} radius of a Gaussian beam). A complete calculation for a fringe pattern having a Gaussian envelope shows that the relative accuracy for the half-time of diffusion is $\sim N^{-2}$ (to be published elsewhere). For the present discussion, we have neglected the effect that a limited number of interference fringes has on the calculations.

When applying equation (10) to experimental situations, several limiting cases can be recognized. If the term $\cos(\phi)$ is constant, the only time dependence in $F(t)$ comes from the relaxation term $\exp(-Dq_0^2 t)$, and this gives a direct measurement of the diffusion coefficient D of the fluorescent molecule. However we see from Figure 2, that for small K (weak bleaching efficiency), the relaxing amplitude $A_1(K, 0)$ can be very small as compared to the constant term $A_0(K, 0)$. In order to remove this latter, we modulated the term $\cos \phi$. Figure 3 shows the fluorescence recovery for $\phi = 0$ (bottom curve), for $\phi = \pi$ (upper curve) and for ϕ varying periodically between 0 and π . Thus, using this approach, one can measure the amplitude (proportional to $A_1(K, 0) \exp(-Dq_0^2 t)$) of an alternating signal of known frequency. Such a phase modulation allows the recording of only the relaxing part of the fluorescence concentration profile.

Sinusoidal modulation of the phase and influence of a flow velocity. Practically, the fringe pattern can be shifted by a controlled mechanical sine vibration of a mirror which is driven in a direction normal to its surface. Therefore, we set $\phi(t) = u \sin(\omega t) + \phi_0$, where u is related to the amplitude of the oscillating mirror and ϕ_0 represents an additional constant fringe pattern shift. It is worth noting that a uniform flow velocity gives a linear displacement of the periodic fluorescence concentration profile. Furthermore, it can be demonstrated that a uniform flow results finally in the following definition for ϕ_0 :

$$\phi_0 = \vec{V} \cdot \vec{q}_0 t.$$

Taking account of both diffusion and uniform flow, the fluorescence signal is then proportional to:

$$A_0(K, 0) + A_1(K, 0) \exp(-Dq_0^2 t) \cos(u \sin \omega t + \vec{V} \cdot \vec{q}_0 t).$$

This signal can be decomposed into a harmonic series with respect to the fundamental modulating frequency ($\omega/2\pi$) of the modulation:

$$F(t) = \sum_{n=0}^{n=\infty} [f_{2n}(t) \cos(2n\omega t) + f_{2n+1}(t) \sin((2n+1)\omega t)]$$

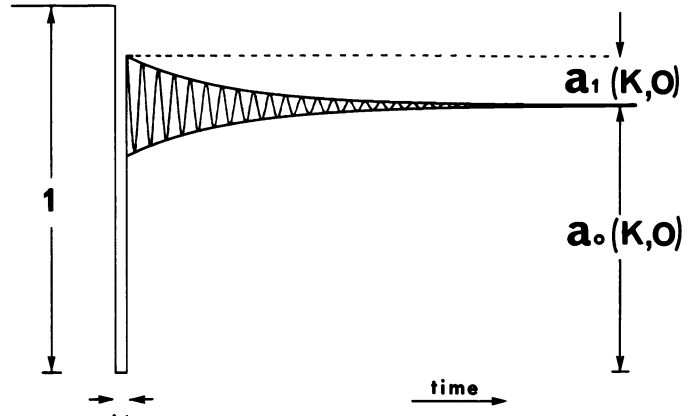


Fig. 3. Theoretical fluorescence recovery signal as a function of time as monitored by an attenuated fringe pattern (periodicity i) produced by two interfering laser beams. The bottom continuous line corresponds to a phase difference between the two beams $\phi = 0$, the upper curve to $\phi = \pi$, while the wavy line corresponds to a periodic variation of $\phi(t)$ with time. The modulated part of the signal is proportional to $A_1(K, t)$ (amplitude of the Fourier component of the concentration of fluorophores at $q_0 = 2\pi/i$) while the d.c. part is proportional to the average concentration of fluorescent molecules $A_0(K, 0)$.

where:

$$\begin{aligned} f_{2n}(t) &= 2A_1(K, 0) J_{2n}(u) \exp(-Dq_0^2 t) \cos(\vec{V} \cdot \vec{q}_0 t); \quad (n \neq 0) \\ f_{2n+1}(t) &= 2A_1(K, 0) J_{2n+1}(u) \exp(-Dq_0^2 t) \sin(\vec{V} \cdot \vec{q}_0 t); \\ f_0(t) &= A_0(K, 0) + A_1(K, 0) J_0(u) \exp(-Dq_0^2 t) \cos(\vec{V} \cdot \vec{q}_0 t) \quad (11) \end{aligned}$$

with the Bessel function $J_n(u)$. Three independent variables are accessible simultaneously in one experiment: the time independent component $f_0'(t) = f_0(t) - [J_0(u)/(2J_2(u))] f_2(t)$, the odd and even harmonic components, respectively $f_1(t)$ and $f_2(t)$. As a consequence of the modulation of the fringe pattern position, one can easily measure transport coefficients (lateral diffusion coefficient and uniform flow velocity), using the mean level of fluorescent light as an independent control.

Curve fitting and determination of transport coefficients. In the absence of flow, the semilogarithmic plot of $f_2(t)$ displays an exponential decay characterised by $\tau^{-1} = Dq_0^2$ (see Figure 4), giving $D = i^2/4\pi^2\tau$. The asymptote will provide the immobile fraction, if this is absent, $f_2(t)$ should relax to the zero level. Multiple diffusional kinetics can be determined with the usual restriction concerning the analysis of a sum of exponential decays.

The presence of a constant flow velocity introduces an additional modulation in the amplitude of the two terms $f_1(t)$ and $f_2(t)$, as schematically illustrated in Figure 4. The flow velocity V can be deduced from the time difference between two maxima: $t = 2\pi(\vec{q}_0 \cdot \vec{V})^{-1}$ for $\vec{q}_0 \cdot \vec{V} > Dq_0^2$. Even a very slow directional flow ($\vec{q}_0 \cdot \vec{V} < Dq_0^2$) can still be measured from the ratio $\frac{f_1(t)}{f_2(t)} = \frac{J_1(u)}{J_2(u)} \tan(\vec{V} \cdot \vec{q}_0 t) \cong \frac{J_1(u)}{J_2(u)} \vec{V} \cdot \vec{q}_0 t$. Simultaneously the diffusion coefficient D can be deduced from the time dependence of the quantity:

$$f_2(t) + \left(\frac{J_2(u)}{J_1(u)}\right) f_1(t) = [J_2(u) \exp(-Dq_0^2 t)]^2$$

The above expression yields a measurement of lateral diffusion under the condition $V \ll DN^2/w$ where N is the total number of fringes in the beam size w . Otherwise, the flow over the fringe pattern would move the bleached sample

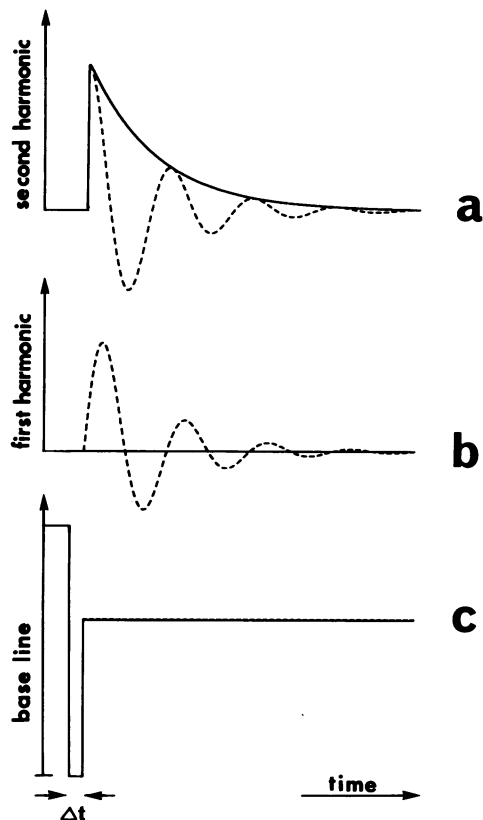


Fig. 4. Harmonics of the fluorescence signal for a sinusoidal phase modulation $\phi(t) = u \sin \omega t$, at the frequency ω/π (curve a), $\omega/2\pi$ (curve b) and 0 (curve c). The dotted line on each curve represents the signal produced by superposition of flow and Brownian diffusion. These three curves are processed from the fluorescence recovery signal depicted in Figure 3.

volume to a non-illuminated area. The linear plot of τ versus i^2 is considered as an essential proof of a random diffusion process over the spatial range that is experimentally accessible.

The inverse plot of τ^{-1} versus i^{-2} is also very instructive since the lateral diffusion coefficient can be measured from a linear regression with a slope of $4\pi^2 D$. For example, one can eliminate spurious effects which are caused by reversibility of the bleaching. The time constant, τ_{rev} , gives a non-zero ordinate intercept of the linear regression:

$$(\tau)^{-1} = (\tau_{rev})^{-1} + 4\pi^2 D(i)^{-2}$$

Additionally, very small flows and/or diffusion in limited space can be readily detected by these linear plots.

Signal to noise ratio and sensitivity.

An important parameter required for evaluating the performance of the experimental set-up is the signal-to-noise ratio S/N . The phase modulation $\phi(t)$ suppresses all the contributions to the noise that are not correlated to the modulation, such as noise associated with mechanical vibrations of the different optical components, black current of the photomultiplier, etc. The principal contribution to the noise comes from the Poisson statistics over the total number of cathode photoelectrons collected during a given time period. Then:

$$S/N = \frac{B \cdot A_1(K, o)}{[B \cdot A_0(K, o)]^{1/2}} = (B/I_1(K))^{1/2} \exp(-K/2) I_1(K) \quad (12)$$

The dotted line in Figure 2 represents S/N as a function of K (with $B = 1$). We see that it becomes relatively flat for $K \geq 2$.

The proportionality factor B takes into account the efficiency of the fluorescence collection, the efficiency of the photocathode, and the monitoring light intensity (I_0). It is also proportional to the overall number of fluorescent molecules within the planar fringe pattern volume. Therefore, the signal-to-noise ratio is enhanced by spatial averaging of the diffusion kinetics over a large sample volume.

Another estimate of the sensitivity of the method can be found from the ratio of the modulated fluorescence intensity to the bleached fluorescence intensity. For example, considering first order photobleaching kinetics, we have:

$$\rho = \frac{A_1(K, o)}{I - A_0(K, o)} = \frac{\exp(-K) I_1(K)}{I - \exp(-K) I_0(K)}$$

For small K ($K < 0.1$) this becomes $\rho = 1/2$, showing that the amplitude of the time dependent fluorescence recovery signal equals one half of the average number of bleached molecules for an ideal instrument. In practice, ρ has to be considered as a criterion of sensitivity for the whole set-up because it tests the contrast of the interference fringes, their correct localisation in the observed sample volume, and the collection of fluorescence light. This parameter must be maximized if one is to extract the greatest amount of information from the profile of photobleached molecules.

Experimental results

As a test of theoretical results, a solid sample (FITC in epoxy resins) was made. After applying the bleaching pulse, a fixed concentration profile of fluorophores is produced in the test sample. The amplitude of the modulation (a.c. voltage applied on the ceramic) was adjusted. The maximum amplitude for the modulated signal (second harmonic $f_2(t)$), was reached when $J_2(u) = 0.48$ for $u = 3.05$. The results from this experiment were compared with the curves shown in Figure 4. Producing slow linear shift of the fringe pattern while observing the bleached pattern simulates an artificial opposite uniform flow and modulates the in-phase first harmonic and out-of-phase second harmonic, respectively $f_1(t)$ and $f_2(t)$ of respective amplitudes $2J_1(u)$ and $2J_2(u)$.

For the BSA in water-glycerol solutions (15/85 w/w) a typical $f_2(t)$ curve obtained in one run is shown in Figure 5a. The interfringe spacing was $i = 51 \mu\text{m}$, the equivalent concentration of FITC, 10^{-6} M. An exponential relaxation was well observed, as evidenced by the corresponding semi-logarithmic plot of Figure 5b. From this linear plot we extracted the characteristic relaxation time:

$$\tau = (Dq_0^2)^{-1} = 98.7 \text{ s}$$

The experiment has been repeated for different interfringe spacings i . When the corresponding relaxation times were plotted as a function of i^2 (Figure 6), then τ was found to be linear with respect to i^2 , and the linear regression line crosses the origin. This is characteristic of a single diffusion of irreversibly bleached fluorophores. The corresponding diffusion coefficient of FITC-BSA is $D = 6.7 \times 10^{-9} \text{ cm}^2/\text{s}$ (room temperature) in good agreement with the literature data (Tanford, 1961).

These data were obtained with a bleaching pulse of 580 ms duration, having 0.3 W incident power on the sample ($w = 0.7 \text{ mm}$): the bleaching efficiency, under these conditions, was small ($K = 0.15$). For the first order bleaching kinetics, the expected sensitivity criterion was $\rho = 0.5$ which is in good agreement with the observed ratio of the modulated amplitude over the bleached fluorescence intensity (0.4).

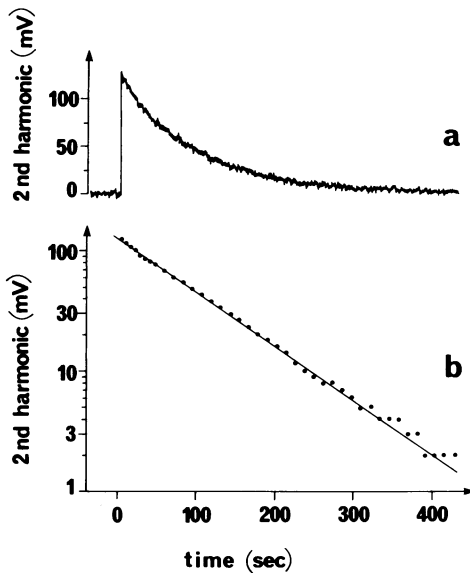


Fig. 5. Recording of the second harmonic modulated fluorescence recovery signal (top curve) for a FITC-BSA, water-glycerol solution. The equivalent concentration of FITC is 10^{-6} M. The incident power used in the bleaching pulse (580 ms duration) was 0.3 W (sinusoidal modulation of the phase $\phi(t) = u \sin \omega t$, $\omega/2\pi = 430$ Hz). Bottom curve is a semi-logarithmic plot of the data points shown in the top curve. The exponential decay is well defined and has a characteristic relaxation time of 98.7 s.

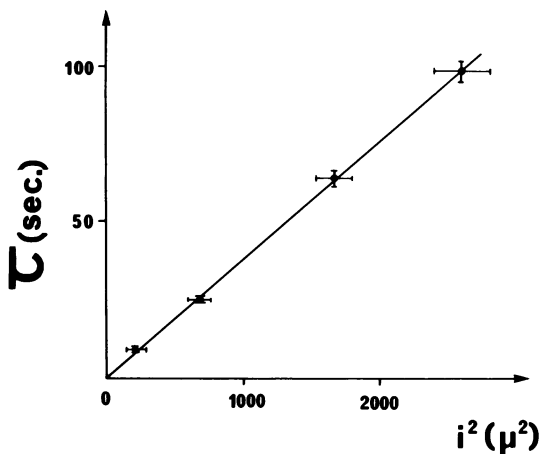


Fig. 6. Characteristic decay time of FITC-BSA in water-glycerol solution as a function of the square of the interfringe spacing i^2 . The slope gives a diffusion coefficient, $D = 6.7 \times 10^{-9}$ cm²/s.

To test if heating of the sample during the bleaching pulse affected the result, several experiments were performed with decreasing FITC concentrations (from 10^{-6} to 10^{-8} M). The optical densities of the samples at 488 nm were in the range 10^{-2} – 10^{-4} . An estimation of the extent to which the temperature rose during the bleaching pulse gives a value of 0.1°C for the more concentrated solution and 10^{-30} °C for the less concentrated. However, we were not able to find any change in the measured diffusion coefficient.

Discussion

Comparison with other methods

We describe a method of fringe pattern photobleaching associated with optical signal processing of the recovery of the modulated fluorescence. The sine profile of the light in-

tensity solves the mass diffusion equation (1) in its adequate Fourier space. The modulation eliminates the base line arising from the mean light intensity and the mean fluorophore concentration. Hence, the method is formally equivalent to the Forced Rayleigh light scattering technique that has been developed for accurate measurement of mass diffusion coefficients (Rondelez *et al.*, 1978; Leger *et al.*, 1981).

In principle, any imaging system of an initially non-homogeneous distribution of molecules can be used to measure transport coefficients. A multipoint analysis (Koppel, 1979), or the image analysis after periodic pattern photobleaching (Smith *et al.*, 1979) illustrate the interest in sensitive imaging devices. They can be combined with a static fringe pattern photobleaching, as recently published (Weiss *et al.*, 1982). A photomultiplier, that collects fluorescent light under sinusoidal excitation, performs the same function. In a similar approach (Wang *et al.*, 1982), the specimen is illuminated by a series of parallel stripes that can be translated back and forth.

Application to biological macromolecules

The fringe pattern combines the advantages of high sensitivity with an adjustable scale length. The actual sensitivity of the method depends upon the overlapping volume of the two beams, the collection angle, and photomultiplier quantum yield. Therefore, the same absolute number of detectable fluorophores (10^3 – 10^4) as used in the conventional spot photobleaching method could be diluted over a large volume, provided this matched requirements of the fringe pattern. A lower density of bleaching light (30 W/cm² for 300 ms) can reduce the damage to the sample. The use of a collecting lens having a high numerical aperture gives the opportunity to study plasma membrane proteins such as hormone receptors localized on the cell surface and labelled with fluorescent ligands (Schlessinger *et al.*, 1978). We can also examine dispersions of membrane fragments provided they are larger than the interfringe. The modulated amplitude of the fluorescence recovery displays a single exponential decay per diffusional component which is quantitative even with a small number of fringes (~ 10). For a lower number, the method gives the order of magnitude of the transport coefficients together with their qualitative variation following a biochemical modification of the preparation.

We measure one component of the Brownian diffusion tensor averaged over a large volume while the spot photobleaching method performs locally the measurement of the mean diffusion coefficient on a given membrane surface. The scale, i , over which the motion is followed can easily be varied from 50 μ m down to the wavelength of light (0.5 μ m) and this is only limited by diffraction. These characteristic distances are determined completely by the sinusoidal profile of light, and are independent of the bleaching conditions. For diffusion measurements, the verification of the proportionality between the inverse relaxation time τ^{-1} and i^{-2} provides a direct route for discriminating between true Brownian diffusion and relaxation by any other process (convection, reversible photobleaching). The initial bleaching light intensity does not contribute to the relaxation kinetics, therefore, multi-exponential decays and immobilized fractions can be accurately analysed. The latter gives a modulated fluorescence recovery signal of a constant amplitude (as observed for FITC embedded in epoxy resins).

Other possible developments are the study under a microscope of the transport of cellular elements such as plasma

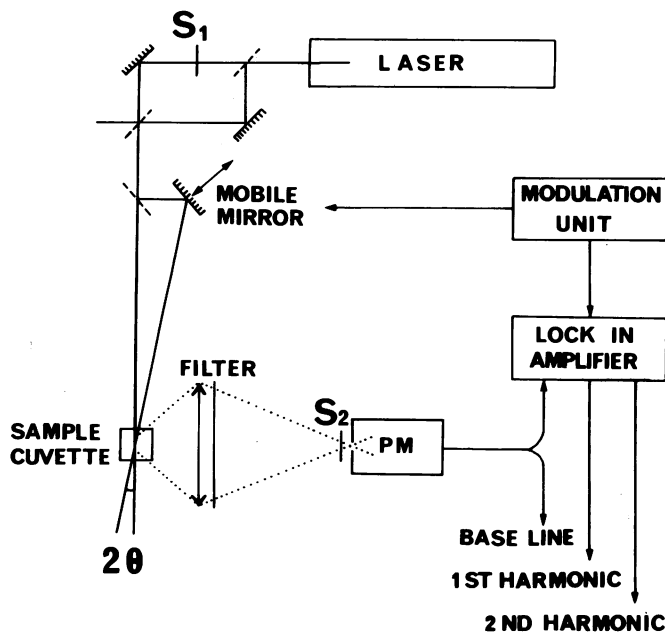


Fig. 7. Schematic block diagram of the equipment. A 165-08 Spectra Physics Argon laser is used to generate light of the $\lambda_0 = 488$ nm line. The 10^{-4} attenuation between bleaching and observation beam is made by the Mach-Zehnder interferometer. Bleaching and monitoring beams are thus interferometrically aligned. A second interferometer produces a sinusoidal light intensity profile in the sample cell. The interfringe spacing i is variable between 0.5 and 100 μm and the desired spacing is selected by varying the distance between the beam splitter and the mobile mirror, the position of which can be modulated further ($\pm \frac{\sqrt{2}}{2} \lambda_0$) by the excitation of a piezoelectric ceramic. The fluorescence intensity is collected through a lens, filtered and focussed on the shutter S_2 ; the modulation of the ceramic, gives the reference frequency of the lock-in-amplifier.

membrane components and cytoplasmic proteins. The very large depth of focus of the fringe pattern provides a versatile tool in studying the transport properties of fluorescent macromolecules. The method is naturally compatible with the study of transport and/or polymerization phenomena in bulk solution of molecules of biological interest.

Materials and methods

FITC was conjugated to BSA (according to the procedure of Stacey and Allfrey, 1977), with the following modification: the final dialysis step was performed against phosphate buffered saline 0.1 M, pH 7.4, containing 10 g/l of lipid-free BSA, to eliminate the possibility of FITC being only adsorbed and not covalently bound on the protein. Solutions of H_2O /glycerol, 15/85 (w/w), containing 10^{-6} – 10^{-8} M of FITC-BSA were gently mixed for 48 h before use.

The optical and electronic set-up is schematically represented in Figure 7. A Mach-Zehnder interferometer is used to split the incident laser beam (in TEM 00 mode, wavelength 488 nm) into two parts. The first part (bleaching beam) may be interrupted by the mechanical shutter S_1 , while the second part (observation beam) is attenuated by a factor 10^4 by successive reflections on appropriately coated surfaces ($\sim 1\%$ reflection). The two laser beams are then recombined. The correct alignment of the beam is checked on the orthogonal output of the interferometer, where the two beams are equally attenuated (1%). Any misalignment in the angle α yields a typical fringe pattern in the cross section of the two beams. The alignment is estimated to be correct when the typical ring-like structure is observed on a far screen. The residual misalignment of the angle of two coherent beams of radius $w = 1$ mm is less than $\lambda/(2\pi w) \cong 10^{-4}$ rad. The beam then passes through a second interferometer, constructed from a 50% beam-splitter and a mobile mirror mounted on a piezoelectric ceramic. The two outgoing beams are recombined in the sample. Planar interferences are produced in the volume of the overlapping beams. A displacement of $\lambda_0\sqrt{2}/2$ of the mobile mirror in a direction normal to its surface shifts the fringe pattern by $i/2$, while the resulting lateral

displacement of the beam has a negligible influence on the modulated fluorescence signal. The fluorescent light is collected through lenses (solid angle of order $0.5/4\pi$ sterad) and interrupted by shutter S_2 during the bleaching pulse.

The modulation unit controls the shutter position and the mirror-piezoelectric ceramic assembly. In order to deliver the bleaching pulse, S_1 must be left open for a time which can be adjusted between 10 and 800 ms, at the same time S_2 is closed: during this period the piezoelectric is not activated. During the observation period of the experiment S_1 is closed, S_2 open, the position of mirror M_1 is modulated and data is collected.

The signal from the photomultiplier is fed to a programmable double phase lock-in-amplifier (ATNE) and a digital memory oscilloscope (Tektronix).

Measurement of interfringe spacing

The interfringe spacing is related to the angle 2θ between the two interfering beams by $i = \frac{\lambda_0}{2\sin\theta}$. It can be measured either directly from the half angle θ ,

or through the projection of the fringe pattern on a far screen using a high magnification microscope objective: the latter procedure gives greater accuracy. Typically, the relative uncertainty on i is of order 2%, and this results in the same uncertainty on q_0 .

Acknowledgements

We gratefully acknowledge Dr.G.Guillot and Dr.H.Hervet for their stimulating contribution to this work, Dr.R.Wijnaendts van Resandt, Professor K.Simons, and Dr.P.Spragg for critically reading the manuscript, and Ines Benner for typing it. This work was supported by research grants from the Centre National de la Recherche Scientifique (ERA 690 and ERA 542), the Délégation Générale à la Recherche Scientifique et Technique, and the Université de Paris VII.

References

- Axelrod,D., Radvin,P., Koppel,D.E., Schlessinger,J., Webb,W.W., Elson,E.L., and Podleski,T.R. (1976a) *Proc. Natl. Acad. Sci. USA*, **73**, 4594-4598.
- Axelrod,D., Koppel,D.E., Schlessinger,J., Elson,E., and Webb,W.W. (1976b) *Biophys. J.*, **16**, 1055-1069.
- Dragsten,P., Henkart,P., Blumenthal,R., Weinstein,J., and Schlessinger,J. (1979) *Proc. Natl. Acad. Sci. USA*, **76**, 5163-5167.
- Edidin,M., Zagayanski,Y., and Lardner,T.J. (1976) *Science (Wash.)*, **191**, 466-468.
- Koppel,D.E. (1979) *Biophys. J.*, **28**, 281-292.
- Lanni,F., Taylor,D.L., and Ware,B.R. (1981) *Biophys. J.*, **35**, 351-364.
- Leger,L., Hervet,H., and Rondelez,F. (1981) *Macromolecules*, **14**, 1732-1738.
- Matlin,K.S., Reggio,H., Helenius,A., and Simons,K. (1981) *J. Cell Biol.*, **91**, 601-613.
- Peters,R. (1981) *Cell Biol. Int. Rep.*, **5**, 733-760.
- Peters,R., Peters,J., Tews,K.H., and Bahr,W. (1974) *Biochem. Biophys. Acta*, **367**, 282-294.
- Rondelez,F., Hervet,H., and Urbach,W. (1978) *Chem. Phys. Lett.*, **53**, 138-143.
- Schindler,M., Koppel,D.E., and Sheetz,M.P. (1980) *Nature*, **283**, 346-350.
- Schlessinger,J., Shechter,Y., Cuatrecasas,P., Willingham,M.C., and Pastan,I. (1978) *Proc. Natl. Acad. Sci. USA*, **75**, 5353-5357.
- Schwartz,L. (1965) in *Methodes Mathematiques pour les Sciences Physiques*, published by Hermann, Paris.
- Smith,B., Clark,W.R., and McConnell,H.M. (1979) *Proc. Natl. Acad. Sci. USA*, **76**, 5641-5644.
- Smith,B., and McConnell,H.M. (1978) *Proc. Natl. Acad. Sci. USA*, **75**, 2759-2763.
- Stacey,D.W., and Allfrey,V.G. (1977) *J. Cell Biol.*, **75**, 807-817.
- Tanford,C. ed. (1961) *Physical Chemistry of Macromolecules*, published by John Wiley and Sons, Inc., NY/London.
- Wang,Y., Lanni,F., McNeil,P., Ware,B.R., and Taylor,D.L. (1982) *Proc. Natl. Acad. Sci. USA*, **79**, 4460-4464.
- Weiss,R., Balakrishnan,K., Smith,B., and McConnell,H. (1982) *J. Biol. Chem.*, **257**, 1440-1445.
- Wojcieszyn,J.W., Schelegel,R.A., Wu,E.S., and Jacobson,K.A. (1981) *Proc. Natl. Acad. Sci. USA*, **78**, 4407-4410.